Sensitive detection of cardiac biomarkers using a magnetic microbead immunoassay

Christine F. Woolley and Mark A. Hayes*

To achieve improved sensitivity in cardiac biomarker detection, a batch incubation magnetic microbead immunoassay was developed and tested on three separate human protein targets: myoglobin, heart-type fatty acid binding protein, and cardiac troponin I. A sandwich immunoassay was performed in a simple micro-centrifuge tube allowing full dispersal of the solid capture surface during incubations. Following magnetic bead capture and wash steps, samples were analyzed in the presence of a manipulated magnetic field utilizing a modified microscope slide and fluorescent inverted microscope to collect video data files. Analysis of the video data allowed for the quantitation of myoglobin, heart-type fatty acid binding protein and cardiac troponin I to levels of 360 aM, 67 fM, and 42 fM, respectively. Compared to the previous detection limit of 50 pM for myoglobin, this offers a five-fold improvement in sensitivity. This improvement in sensitivity and incorporation of additional markers, along with the small sample volumes required, suggest the potential of this platform for incorporation as a detection method in a total sample analysis device enabling multiplexed detection for the analysis of clinical samples.

Introduction

Due to their high sensitivity, biosensors have become a popular diagnostic tool for both early and rapid disease detection. Early detection is particularly important in cases of acute myocardial infarction (AMI) where prompt diagnosis is crucial for patient survival. The biomarker targeted by the biosensor is of key importance and the characteristics an ideal cardiac marker have recently been defined.[1] These criteria include both the rapid release of the biomarker into the blood for early detection and prolonged elevation for later assessment and confirmation. Additionally, the quantitative assay must possess a high clinical sensitivity and specificity. The American College of Cardiology (ACC) and the American Heart Association (AHA) currently recognize a biomarker panel composed of myoglobin, cardiac troponin I (cTnI), and creatine kinase MB (CK-MB) for the diagnosis of AMI.[2,3] However, because CK-MB has a low sensitivity for AMI within six hours after an incident and cTnI is better at detecting minor cardiac damage, CK-MB was not evaluated in this study.[2] Instead, heart-type fatty acid binding protein (H-FABP) was included due to its early release following cardiac injury and diagnostic potential when used as part of a panel with cTnI.[4–7]

Myoglobin is an oxygen-binding protein found in both cardiac and striated muscle, and is currently used as a routine biomarker for AMI.[8,9] Its early release into the blood (increasing 1–3 hours within the onset of myocardial necrosis), as well as relatively high plasma reference concentration (34 μg L^{-1}) illustrate several of the qualities desired in an ideal cardiac marker.[9] However, because it may also indicate skeletal muscle damage, by itself myoglobin has shown a sensitivity of 75.9%, and a clinical specificity of only 25.0% for AMI diagnosis. In recent years H-FABP has also shown promise as an early cardiac injury marker in plasma.[4,7,10,11] Due to its lower concentration in skeletal muscle compared to myoglobin, rapid release into circulation, and potential to predict patient prognosis, H-FABP has received considerable attention.[5–7,12,13] Still, because of its release in other medical conditions, H-FABP alone shows only a 64% sensitivity.[5,14] While no single marker has shown adequate diagnostic accuracy for AMI, a high sensitivity and specificity has been achieved using myoglobin and H-FABP as part of a biomarker panel along with cTnI.[5,8,10,12,14–16] Even with the use of biomarker panels, there exists a need for more sensitive assays capable of rapid analysis for the evaluation of serial measurements to be practical in a clinical setting. This capability would be beneficial not only in the diagnosis of AMI, but for the early detection of many diseases which could greatly improve prognoses.

Over the last few years a great deal of research has been devoted to the development of micro-immunoassay platforms allowing for the sensitive quantitation of varied target biomarkers.[17–25] A particularly interesting subset of this research incorporates the use of magnetic micro- or nano-particles as the solid surface employed for primary antibody fixation and target trapping.[26–34] Use of magnetic particles permits easy sample manipulation and separation from interfering species, as well as straightforward coupling to signal amplification and signal processing.

Department of Chemistry and Biochemistry, Arizona State University, Tempe, Arizona 85287-1604, USA. E-mail: mhayes@asu.edu; Fax: +480-965-2747

This work describes the development of a micro-immuno-assay platform that allows extremely sensitive quantitation. Unique to this technique among magnetic microbead immunoassays is the manipulation of the solid capture surface during data capture. Incorporation of a periodic fluctuation into the observed fluorescence aids in the identification and quantification of the specific signal. This reduces the impact of background fluorescence on quantitative abilities and enables increased sensitivity compared to previous results. This system directly and indirectly addresses many the six metrics of an optimized immunoassay: increased sensitivity, reduced analysis time, reduced cost, lower sample volumes, ability to multiplex and operational simplicity.[35] This work has focused on the optimization of assay features enabling high quantitative sensitivity using small sample volumes and the first steps toward multiplexed detection. Analysis times have been reduced and could be shortened further through incorporation onto a microdevice. Through clinical samples have not yet been evaluated using this technique, these samples cannot effectively be tested until the improvements to the metrics of an optimized assay addressed in this work have been achieved. While the studies here are performed on an AMI biomarker panel composed of myoglobin, cTnI and H-FABP, this format is easily adaptable to the detection of limitless targets and may be incorporated as a detection method into a micro-total analysis system (μTAS) for the parallel detection and quantification of biomarker panels.

Experimental

Myoglobin detection antibody conjugation to fluorescein-5-EX, succinimidyl ester

Fifty micrograms (50 μL; 1 mg mL^{-1}) of polyclonal rabbit anti-human myoglobin reconstituted in DI H$_2$O (LSBio, Seattle, Washington) was added to 50 μL of 1 M sodium bicarbonate in a 1.5 mL capped vial. One milligram of fluorescein-5-EX, succinimidyl ester (FEXS, Invitrogen) was dissolved in 0.1 mL dimethyl sulfoxide (DMSO) and added dropwise to the polyclonal antibody (Pab) solution at room temperature. This was reacted in darkness at room temperature for 3 hours on a stir plate (Corning) and then placed at 4 °C to continue the reaction overnight. The crude reaction mixture was added to a purification column with a 15 000 dalton molecular weight cut-off (Invitrogen). The fluorescently labeled antibody was separated on-column from unbound dye using 10 mM PBS with 0.15 M NaCl and 0.2 mM NaN$_3$, pH 7.2 and collected in a single fraction. The purified FEXS-Pab solution was analyzed for absorbance measurements at 280 and 494 nm (BioTeck Synergy HT Multi-Mode Microplate Reader). These measurements were used to determine the quantity of antibody present and extent of FEXS conjugation.[36]

cTnI and H-FABP detection antibody conjugation to NHS-Fluorescein

For the detection of cTnI and H-FABP, 250 μg (250 μL; 1 mg mL^{-1}) of polyclonal goat anti-human cTnI and 100 μg (100 μL; 1 mg mL^{-1}) polyclonal rabbit anti-human FABP were used as purchased in PBS buffer (cTnI: 0.1% NaN$_3$; FABP: 0.02% NaN$_3$,

0.1% BSA), pH 7.2. NHS-Fluorescein (Thermo Scientific) was dissolved in DMSO to a concentration of 10 mg mL^{-1} and added dropwise to the Pab solutions at room temperature (24 μL and 40 μL, respectively). This was reacted in darkness at room temperature for two hours on a shaker (Southwest Science LabMini MiniMixer). The crude reaction mixtures were added to dialysis cups (Thermo Scientific) with a molecular weight cut-off of 3500 daltons. The labeled protein was dialyzed in 100 mM PBS with 0.02% NaN$_3$ and 0.1% Tween-20, pH 7.2 overnight. The dialyzed NHS-fluorescein-Pab solutions were analyzed for absorbance measurements utilizing the same method as for anti-human myoglobin Pab.

Preparation of capture antibody and particles

Biotinylated anti-myoglobin monoclonal antibody (bMab; 100 μL; 1.4 mg mL^{-1}; LSBio) was incubated with 3 μL of BioMag paramagnetic particles having an average diameter of 1.6 μm and ranging in diameter from 1.0–2.0 μm (Quagen, Inc.). The total reaction volume was diluted to 300 μL with PBS at pH 7.2 containing 5% BSA, 0.1% Tween-20, and 0.1% NaN$_3$. This was incubated for 3 hours on a shaker (Southwest Science LabMini MiniMixer) at room temperature and then stored at 4 °C until used. Biotinylated anti-cTnI Mab (50 μL, 2 mg mL^{-1}, LSBio) and biotinylated anti-FABP Mab (45 μL, 2.33 mg mL^{-1}, LSBio) were prepared in the same way.

Sandwich immunoassays

Purified human myoglobin (7.33 mg mL^{-1}) was purchased from MyBioSource, LLC (San Diego, California). Standards ranging in concentration from 0.62 fg mL^{-1} to 25 ng mL^{-1} (36 aM to 1.5 nM) were created in buffer through serial dilution of the stock myoglobin. Following sample preparation 30 μL of each Mb standard was mixed with 30 μL of the bMab-BioMag colloid and 5% BSA to prevent non-specific binding. Samples were incubated at room temperature on a shaker for 1 hour. Following the incubation, 4 μL of the detection polyclonal antibody-FEXS solution was added to each sample and incubated in the dark at room temperature for 1 hour with shaking. After the incubation, samples were washed 3 times using 60 μL of PBS buffer and then exchanged to a final volume of 30 μL. Three separate 10 μL droplets were analyzed for each sample, with a total of ten analyses performed for each concentration. Purified human cTnI (1.07 mg mL^{-1}) and H-FABP (2.2 mg mL^{-1}) were purchased from Life Diagnostics (West Chester, Pennsylvania). Standards ranging in concentration from 10 fg mL^{-1} to 10 ng mL^{-1} (0.42 fM to 0.42 nM) for cTnI and from 1 fg mL^{-1} to 10 ng mL^{-1} (67 aM to 0.67 nM) for H-FABP through serial dilution of the initial stock solutions. Following sample preparation samples were prepared and analyzed in the same way as myoglobin.

Data collection

Data were collected using an Olympus IX70 inverted microscope with a charge coupled device (CCD) camera connected to a computer capable of image-capture (Q-Imaging, Surrey, BC). Capture settings for the CCD camera were optimized for the observation of strong fluorescent signal clusters with minimal

contribution from background pixels through studies utilizing biotinylated fluorescein (Sigma-Aldrich) as a positive control. Biotinylated fluorescein was chosen as a control due to the strong binding relationship between biotin and the streptavidin on the BioMag particles and a common fluorophore with the experimental immunoassays. Offset was adjusted to minimize background of a washed sample without reducing pixel intensity from signal; values between −1120 to 440 were tested. With the offset held constant at 100, gain values between 4.7 to 15.0 were explored to maximize the sensitivity of the assay without compromising the dynamic range. Optimal image quality was observed at an offset of 100 and gain of 13.8. Once established, capture settings were held constant for all experiments performed on cardiac targets.

Multiple 10 μL-sized droplets were analyzed for each sample concentration using a microscope slide having a small hydrophilic zone encompassed by a hydrophobic Teflon coating (Tekdon Inc., Myakka City, Florida). A cylindrical rare earth magnet (2.5 cm diameter, 0.3 cm thick) placed 2 cm above the droplet was used to generate the magnetic field (Magcraft, Vienna, VA) and collect structures for ∼30 s. Supraparticle structures approximately 15 μm in length were observed. The magnet was secured to a DC motor by a 7 cm metal shaft allowing for rotation and controlled *via* a USB 4-motor stepper controller (Trossen Robotics). The controller was connected to the motor through a ribbon wire to protect it from fluids used during the experiment. The magnet was rotated at a constant velocity during assays (30 rpm), and illumination from a mercury lamp (Olympus) was passed through the appropriate filter cube and a LCPlanFl 40X/0.60 objective to excite the assay. Emitted fluorescence was collected using the QIACAM FAST cooled Mono 12-bit (QImaging) CCD camera and stored as video files.

Data analysis

Video was analyzed using Image J (National Institute of Health, Bethesda, Maryland). The images (492 × 396) were captured at an exposure time of ∼120 ms (gain, 13.8; offset, 100) which translates to a rate of ∼12 frames per s. Fluorescence intensity measurements were collected by manually selecting all rotors (regions of interest, ROI) within a video frame and summing the fluorescence intensity. This was performed for ten randomized frames per video and the resulting intensities were averaged to attain a single average fluorescence intensity value for a given trial. Ten trials per sample concentration were averaged per experiment.

Results/discussion

Assay optimization and protein detection

Three human cardiac biomarkers, myoglobin, cTnI, and H-FABP, were quantified in buffer using a singleplex immunoassay detection system. Proteins were detected by adjusting the hardware settings such that images with visible, yet unsaturated, signal clusters with minimal background contribution were captured. Using an exposure time of 120 ms, signals generated from low concentrations of proteins (down to 36 aM

of myoglobin) were detected above the background intensity (Fig. 1).

Control experiments were performed at a zero antigen concentration, exposing paramagnetic particles with immobilized capture antibody to fluorescently-labeled detection antibody. Dark structures resulted, with minimal diffuse fluorescence suggesting that little or no nonspecific binding is present. The average fluorescence intensity of the entire image was noted (including pixels from all areas, including diffuse fluorescence between rotors) since distinct signal clusters were not visible. This is a more stringent test for background quantification, since the noise from all pixels is included.

At low sample concentrations, below 360 aM for myoglobin, the signal becomes highly variable and the uncertainty in the measurements was greater than 10%. When the uncertainty in a measurement rises above 10% the signal be detected, but not quantified with a reasonable level of certainty.[37] This distinction is important as it differentiates a qualitative positive result from the ability to distinguish when a biomarker is present in concentrations that correspond to diagnostic cut-off values. For the optimization of a clinical assay it is the quantitation limit that is of interest.

Quantitation limit

Measurements of cardiac targets permitted the quantitation of myoglobin to a minimal concentration of 360 ± 2.5 aM with an observed detection limit of 36 ± 2.5 aM, and a linear standard curve from 360 aM to 14 fM ($R^2 = 0.996$; Fig. 2A). H-FABP and cTnI were quantified to limits of 67 ± 3 fM and 42 ± 0.01 fM, with linear standard curves from 67 fM to 67 pM and 42 fM to 42 pM, respectively ($R^2 = 0.998$; Fig. 2B and $R^2 = 1$; Fig. 2C). The optimized collection of the video sets allowed for improvement in detection over several orders of magnitude compared to previously collected myoglobin data, from 50 pM to 36 aM (Table 1).[30] In addition to approaching these fundamental limits of quantification, the linear range of this method may be easily scaled for the detection of higher concentration samples through the addition of more magnetic microparticles or through sample dilution. The limits of quantitation observed in the present work compare favorably to the metrics of a fully optimized immunoassay, achieving detection on the same order of magnitude as fundamental limitations. At low numbers of molecules, quantification becomes impossible due to Poisson statistics.[37] While targets may be observed below this limit, they may not be quantified due to high levels of uncertainty in the measurements made.

Several differences exist in both the data acquisition and data analysis performed in this work that account for the observed improvement in quantitation ability compared to previous studies.[30] In terms of data acquisition, previous work noted differences in signal strength depending on their location in the field of view, increasing variation in both signal and noise. The changes to optics and acquisition conditions eliminated this issue, producing rotors with similar signal intensities independent of their location. Optimizing acquisition conditions through control studies with b-fluorescein resulted in an
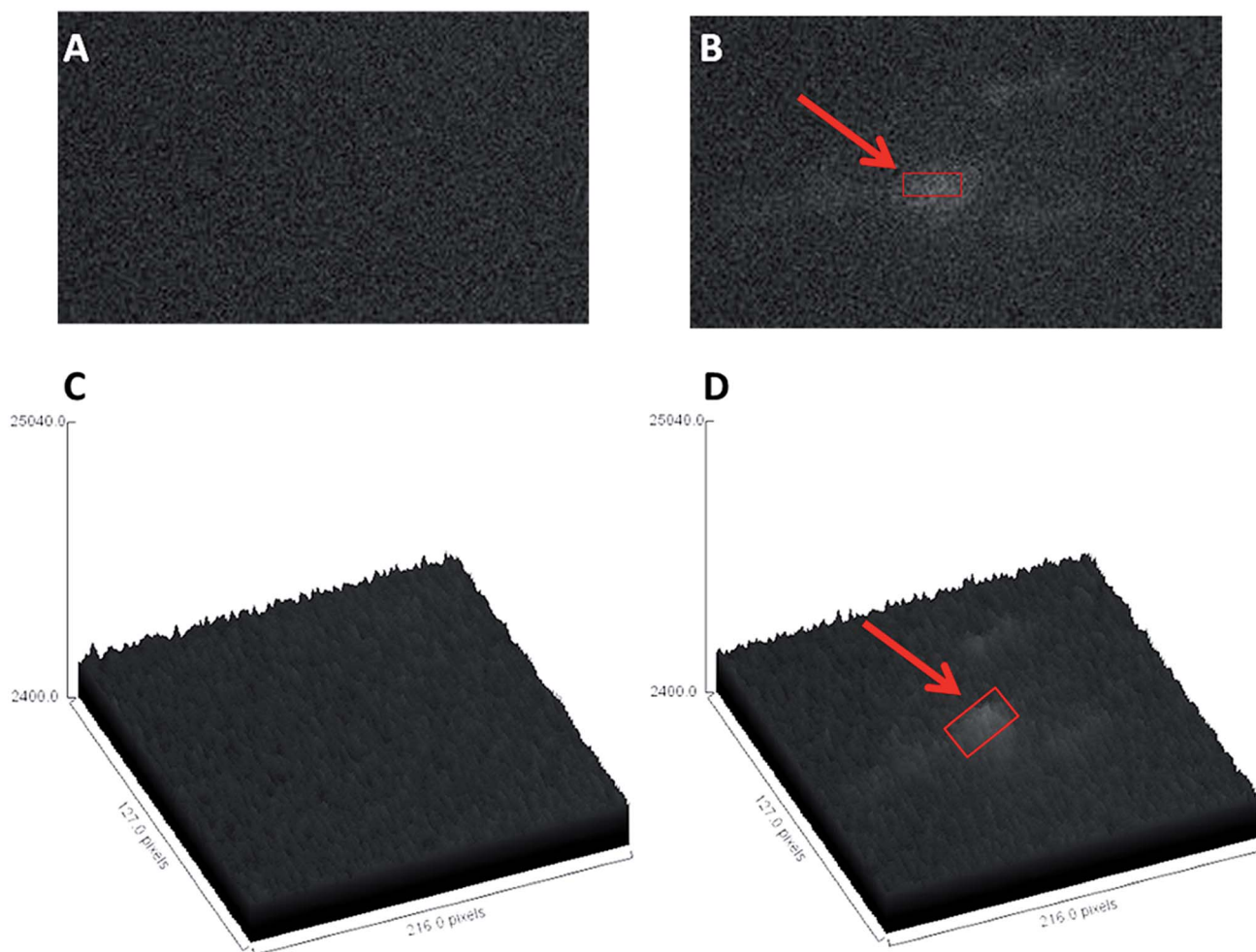
Fig. 1 (A and B) Images showing fluorescence of high sensitivity immunoassays at the detection limit (below the limit of quantification) for 36 aM myoglobin (B) compared to background (A). (C and D) Surface plots illustrating the difference in fluorescence intensity between background (zero concentration, C) and signal clusters representing specific signal (36 aM myoglobin, D). While the signal clusters are not as distinct as those observed for higher target concentrations, this represents the lower limit detectable above zero concentration. Red boxes and arrows indicate the position of the observed signal above background.

increase in exposure time from 50 to 120 ms, as well as reductions in gain (from 2000 to 13.8) and offset (from 2600 to 100).[30] The increase in exposure time still allowed clear visualization of rotor rotation while reducing the impact on noise compared with a shorter exposure. With a lowered gain, the amplification of the image collected by the CCD camera is reduced. Since both the signal and noise are reduced, this lowered value will improve the signal-to-noise ratio (S/N) and reduce the background intensity and noise while specific signal remains visible. By contrast, reducing the offset allows lower intensity values for both specific signal and background fluorescence to be captured. While this increases both the background intensity and noise as well as signal intensity and noise, this minimal value assures that clusters from low signal concentrations may be observed. By improving the signal-to-noise ratio of the captured video files lower intensity signals may be differentiated from background noise, improving assay sensitivity.

Along with the changes made to data acquisition conditions, the process of data analysis has also been altered to increase the signal power obtained from each sample.[30] In previous work a small region of each image (150 × 120 pixels), containing roughly two of the 10–15 signal clusters present overall, was analyzed. Additionally, while signal clusters contributed to less than 30% of the region selected, the average pixel intensity was calculated for the entire selected area, including both signal and noise.[41] Signal processing studies performed on this data conclude that by calculating pixel intensity for the entire image selection, and by only two of the signal clusters contributing to target quantification, a large portion of the signal power is lost while the noise power is increased.[41] By manually segmenting data and selecting all rotors in each frame (492 × 396 pixels) as was done in this work, both issues observed with previous analysis methods are solved. The overall noise power is reduced while signal power is increased.[41] This, coupled to the increase in S/N through optimal data acquisition conditions, allowed for a five-fold improvement in assay sensitivity.

In terms of the mass action equilibrium and detection, sensitivity is maximized by using an excess of both primary and
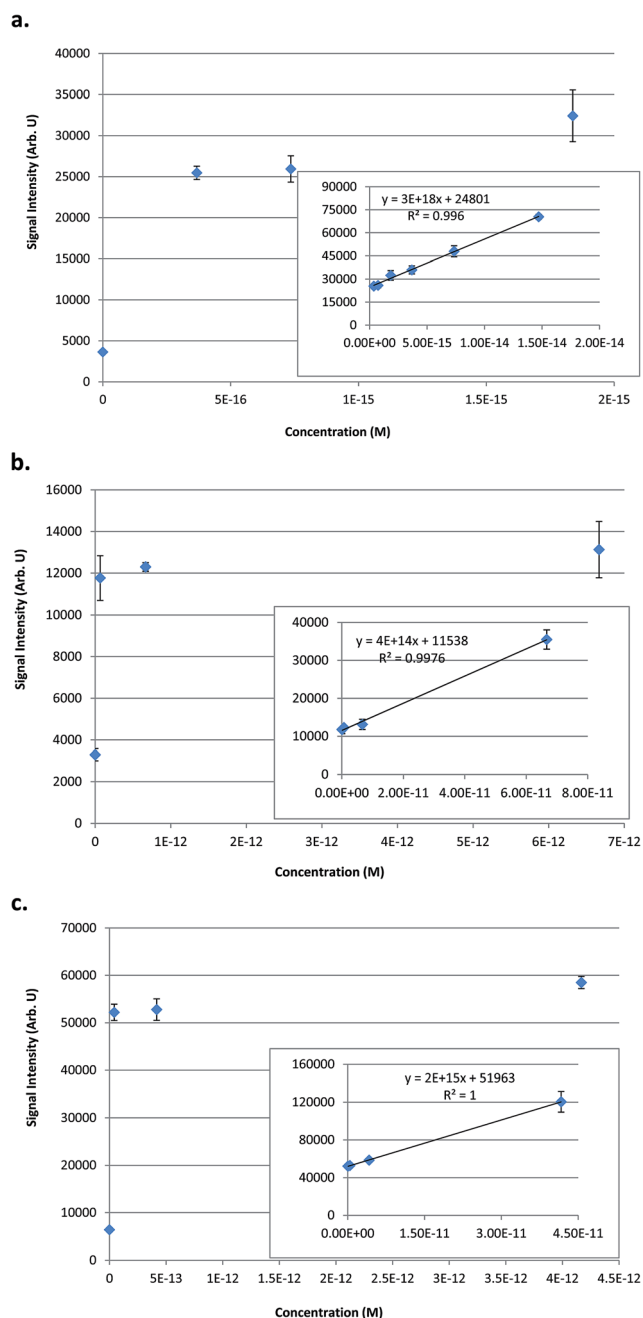
a.

b.

c.

Fig. 2 Standard curves showing signal intensity data for the sandwich immunoassays performed on cardiac biomarker targets. (a) Plot showing the quantitation of myoglobin down to a minimal concentration of 360 aM. Inset shows the linear range to 14.7 fM. (b) Plot showing the quantitation of h-FABP to a minimal concentration of 67 fM with inset showing the linear range to 67 pM. (c) Plot showing the quantitation of cTnI to a minimal concentration of 42 fM with inset showing the linear range to 42 pM.

secondary antibodies, and heavy labeling of secondary antibodies (average among all targets of 4 labels per antibody). Given that the paramagnetic particles have a binding capacity of 8.2 nmol mL^{-1} (manufacturer specifications), the binding capacity for the primary antibody preparation is 82 nM. Using fundamental relationships from basic immunology, the

equilibrium reaction between the protein and primary antibody can be described as

$$K_{eq} = \frac{[AgAb1]}{[Ag][Ab1]} \tag{1}$$

where [AgAb1] is the concentration of bound antigen, [Ag] is the concentration of antigen, [Ab1] is the concentration of primary antibody, and K_{eq} is the equilibrium constant. Given a K_{eq} of 10^9 M^{-1}, the equilibrium concentration of bound antigen for a myoglobin sample at a concentration of 3.6 fM is 0.3 pM, about one hundred times the concentration of target present. A similar calculation can be performed for the reaction of bound antigen with secondary antibody, giving an equilibrium concentration of [AgAb2] in the nM range. With these experimental conditions it can be determined that nearly all antigen is bound in the sandwich immunoassay, resulting in a linear response for the portion of the sigmoidal immunoassay curve examined.

At myoglobin concentrations below 360 aM, uncertainty is too high in the measurement to achieve satisfactory quantitation. Although the lowest concentrations detected could not be quantified due to high variations in signal, the potential exists to improve quantitative sensitivity through coupling to available signal processing approaches.[41] Using this approach, the detection limit of previously published data has been improved by a factor of 100. If the same factor of improvement and reduction in uncertainty for a given sample was realized for the data collected in this work, quantitation of the lowest sample data collected would be possible.

Repeated experiments exhibit a similar result. Fig. 3 shows the average fluorescence intensity of data collected from four separate experiments with independent dilutions of a myoglobin stock sample. Error bars show the standard deviation of each data set. Differences in overall fluorescence intensity were observed between experiments, due to aging of the mercury lamp used to illuminate samples. Even when differences in fluorescence intensity were observed between days, the same linear relationship was observed.

Assay evaluation

As has been noted previously, in static immunoassays background fluorescence is a serious concern that limits the ability to differentiate specific signal from noise. Signal processing strategies offer the potential to improve detection limits through the identification of specific signal generating surfaces and reduction of background elements to reduce the variation observed in signal intensity for low concentration samples.[41] Surface localization is of use in image processing because it creates distinct signal objects that are easier to detect and quantify compared to signal spread over the entire field of view. Creating these distinct signal objects allows for segmentation of collected images and the quantitation of fluorescent species bound in the immunoassay without the influence of diffuse background fluorescence.

The potential to optimize quantitation capabilities also exists through the use of new signal input patterns. Lock-in amplification is a commonly employed method to recognize a specific input signal in the presence of noise.[42] This method allows an

Table 1 Quantitation limits for immunoassay techniques. Optimized values represent the limit to immunoassay quantitation in a 10 μL sample volume

	Previous studies[30]	Commercial techniques[38,39]	Present work	Optimized values	Plasma concentration[40]
Myoglobin	50 pM	1.5 nM	360 ± 2.5 aM	33 aM	2.5 nM
H-FABP	—	6.7 pM	67 ± 3 fM	33 aM	110 pM
cTnI	—	83 pM	42 ± 0.01 fM	33 aM	62.5 pM

input signal modulated in amplitude to be matched to a reference signal with the same periodicity and amplified while background noise is not recognized and is effectively removed. It has been used in previous work to achieve detection limits in the pM range.[30,32] However, because the reference signal generated by lock-in amplification is a sine wave, its correlation with the input wave is imperfect and signal power is lost. This has been addressed in part by the development of a new signal processing method that maintains the input signal modulation but uses a new waveform as the reference signal.[37] While this approach was successful in improving quantitation, using autocorrelation analysis to recognize more complicated input patterns could improve the distinction between signal and noise and increase the slope of the regression line at low sample concentrations.

Other immunoassay techniques have worked on improving quantitative sensitivity for protein targets.[17,23–25,33,34] Compared to those studies that were performed using traditional laboratory equipment,[23–25,33,34] the assay investigated in this work achieved superior sensitivity (aM to fM range compared with typical nM sensitivity) using shorter incubation times. Another study discussed the development of a microchip-based immunoassay for cTnI detection.[17] Movement to the chip format allowed for shorter analysis times and easy adaptability to portable devices and multiplexed analysis. While offering an improvement over this work in terms of analysis time, the sensitivity achieved in this work was superior (fM compared with pM) using a comparable sample volume.

The three biomarker targets evaluated in this work present clinically at levels in the pM–nM range (Table 1).[40] As tested in this work, superior levels of sensitivity, beyond those necessary for clinical diagnostics have been achieved. Testing of increasingly complex samples in plasma or from whole blood could introduce additional matrix effects influencing various aspects of the assay. While additional refinement of the platform may be necessary, achieving high sensitivity in a buffer system represents a necessary first step in an optimized assay design.

Many studies have reported on the improved sensitivity of cardiac diagnostic ability with the use of a biomarker panel as opposed to a single target.[5,8,10,12,14–16] One consequence of this is that parallel detection of targets from a single sample is desirable. Along with the potential to optimize this immunoassay platform for sensitive analyte quantitation, the use of magnetic
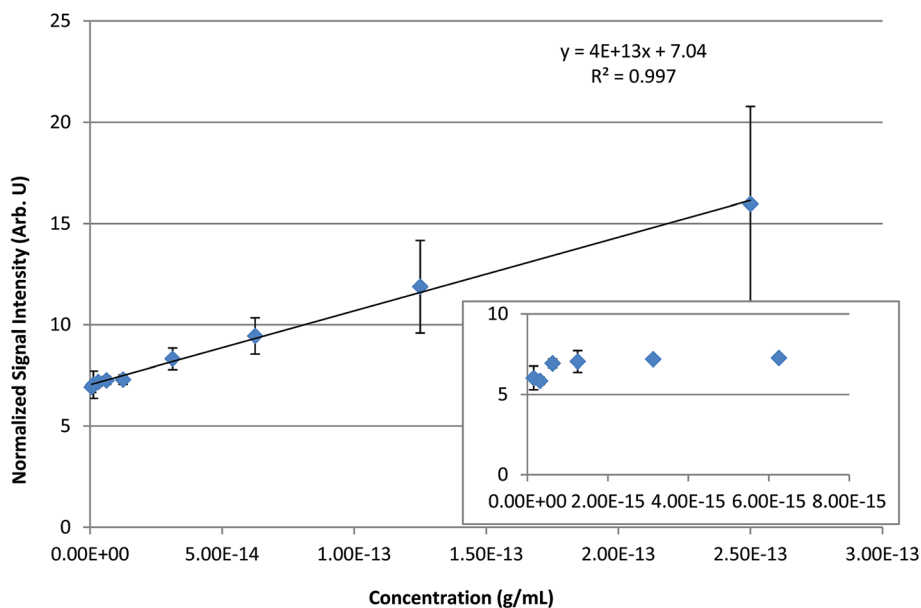
Fig. 3 Standard curve showing the average signal intensity *versus* concentration for the myoglobin sandwich immunoassay for four different experiments using the target protein. The inset shows the lower concentrations on the standard curve, error bars represent the standard deviation among data sets. Signal intensity has been normalized to the background intensity (zero concentration) for each data set.

microparticles offers the ability to move from the batch incubation assay conducted within this work to one performed on a microchip as part of a total sample analysis system. Movement to a microchip would allow the remaining metrics of an optimized immunoassay to be directly addressed. Easy manipulation of the magnetic solid surface through an applied magnetic field allows for the containment of surfaces functionalized for the capture of different targets in separate regions of the microchip. Following target isolation on chip through separation science techniques, individual species may be flushed into appropriate detection chambers and quantified. Use of convective mixing through the manipulation of the microbead surface could aid in rapid analyte capture and greatly reduce analysis times. The linear range of this technique may also be extended through the dilution of samples investigated, or use of smaller sample volumes, allowing the assay to be tailored to meet detection needs as required for diagnostic or disease monitoring purposes.

Conclusions

Dispersed magnetic beads were utilized in a batch incubation format to conduct sandwich immunoassays on three cardiac biomarker targets. Following sample preparation, 10 μL droplets were manipulated through variations in an applied magnetic field, and the periodic change in observed fluorescence was captured as a video file. Analysis of video utilizing Image J allowed the superior detection of myoglobin (360 aM), H-FABP (67 fM) and cTnI (42 fM) compared to previous results. Though not tested using clinical samples, where matrix effects may impact assay features and necessitate additional optimization, this work represents a necessary first step in the design, evaluation and optimization of an immunoassay platform capable of optimized clinical testing. Improvements to the many of the metrics required for an optimized immunoassay have been achieved in this work, and future studies will allow the remaining features to be directly addressed.

Thus, a magnetic bead immunoassay platform was demonstrated utilizing simple batch incubation and a modified microscope slide. This platform has the potential to be incorporated into a full sample analysis chip as a quantification method for biomarker panels while maintaining sensitive detection capabilities, and offers the ability to couple results to more sophisticated signal processing approaches for the detection of low sample concentrations independently from background noise. In its current form this system directly addresses many of the six metrics of an optimized immunoassay. Incorporation of the assay into a μTAS could further these efforts by affording the ability to multiplex and reduce analysis times while maintaining the high sensitivity, low sample volume, and operational simplicity achieved herein.

Abbreviations

AMI	Acute myocardial infarction
CTnI	Cardiac troponin I
H-FABP	Heart-type fatty acid binding protein
Pab	Polyclonal antibody
MTAS	Micro-total analysis system

Acknowledgements

References

1 A. Qureshi, Y. Gurbuz and J. H. Niazi, *Sens. Actuators, B*, 2012, **171–172**, 62–76.

2 ACC and Cardiac Biomarkers, 2014, http://www.acc.org/education-and-meetings/image-and-slide-gallery/media-detail?id=d9c880ce33f3482f993161076a32990a.

3 R. S. Vasan, *Circulation*, 2006, **113**, 2335–2362.

4 A. Kakoti and P. Goswami, *Biosens. Bioelectron.*, 2013, **43**, 400–411.

5 J. Ishii, J. H. Wang, H. Naruse, S. Taga, M. Kinoshita, H. Kurokawa, M. Iwase, T. Kondo, M. Nomura, Y. Nagamura, Y. Watanabe, H. Hishida, T. Tanaka and K. Kawamura, *Clin. Chem.*, 1997, **43**, 1372–1378.

6 C. H. Huang, M. S. Tsai, K. L. Chien, C. Y. Hsu, W. T. Chang, T. D. Wang, S. C. Chen, M. Huei-Ming Ma and W. J. Chen, *Clin. Chim. Acta*, 2014, **435**, 7–13.

7 J. F. Glatz and R. Renneberg, *Clin. Lipidol.*, 2014, **9**, 205–220.

8 S. P. J. Macdonald, Y. Nagree, D. M. Fatovich, M. Phillips and S. G. A. Brown, *Emerg. Med. J.*, 2013, **30**, 149–154.

9 J. Liao, C. P. Chan, Y. Cheung, J. Lu, Y. Luo, G. W. H. Cautherley, J. F. C. Glatz and R. Renneberg, *Int. J. Cardiol.*, 2009, **133**, 420–423.

10 Y. Tonomura, S. Matsushima, E. Kashiwagi, K. Fujisawa, S. Takagi, Y. Nishimura, R. Fukushima, M. Torii and M. Matsubara, *Toxicology*, 2012, **302**, 179–189.

11 K. Inoue, S. Suwa, H. Ohta, S. Itoh, S. Maruyama, N. Masuda, M. Sugita and H. Daida, *Circ. J.*, 2011, **75**, 2813–2820.

12 S. D. Molin, F. Cappellini, R. Falbo, S. Signorini and P. Brambilla, *Clin. Biochem.*, 2014, **47**, 247–249.

13 K. Setsuta, Y. Seino and K. Mizuno, *Int. J. Cardiol.*, 2014, **176**, 1323–1325.

14 C. G. McMahon, J. V. Lamont, E. Curtin, R. I. McConnell, M. Crockard, M. J. Kurth, P. Crean and S. P. Fitzgerald, *Am. J. Emerg. Med.*, 2012, **30**, 267–274.

15 O. V. Gnedenko, Y. V. Mezentsev, A. A. Molnar, A. V. Lisitsa, A. S. Ivanov and A. I. Archakov, *Anal. Chim. Acta*, 2013, **759**, 105–109.

16 R. Body, G. McDowell, S. Carley, C. Wibberley, J. Ferguson and K. Mackway-Jones, *Resuscitation*, 2011, **82**, 1041–1046.

17 S. Y. Song, Y. D. Han, K. Kim, S. S. Yang and H. C. Yoon, *Biosens. Bioelectron.*, 2011, **26**, 3818–3824.

18 S. Casolari, B. Roda, M. Mirasoli, M. Zangheri, D. Patrono, P. Reschiglian and A. Roda, *Analyst*, 2013, **138**, 211–219.

19 J. Tian, L. Zhou, Y. Zhao, Y. Wang, Y. Peng, X. Hong and S. Zhao, *J. Fluoresc.*, 2012, **22**, 1571–1579.

20 D. Lin, J. Wu, M. Wang, F. Yan and H. Ju, *Anal. Chem.*, 2012, **84**, 3662–3668.

21 G. Liang, S. Liu, G. Zou and X. Zhang, *Anal. Chem.*, 2012, **84**, 10645–10649.

22 S. Spindel and K. E. Sapsford, *Sensors*, 2014, **14**, 22313–22341.

23 M. Ammar, C. Smadja, G. T. Phuong, M. Azzous, J. Vigneron, A. Etcheberry, M. Taverna and E. Dufour-Gergam, *Biosens. Bioelectron.*, 2013, **40**, 329–335.

24 M. M. Caulum, B. M. Murphy, L. M. Ramsay and C. S. Henry, *Anal. Chem.*, 2007, **79**, 5249–5256.

25 M. Park, J. H. Bong, Y. W. Chang, G. Yoo, J. Jose, M. J. Kang and J. C. Pyun, *Anal. Methods*, 2014, **6**, 1700–1708.

26 J. Han, J. Zhang, Y. Xia, S. Li and L. Jiang, *Colloids Surf., A*, 2011, **379**, 2–9.

27 G. Proczek, A. L. Gassner, J. M. Busnel and H. H. Girault, *Anal. Bioanal. Chem.*, 2012, **402**, 2645–2653.

28 A. Ranzoni, G. Sabatte, L. J. van Ijzendoorn and M. W. J. Prins, *ACS Nano*, 2012, **6**, 3134–3141.

29 Y. K. Hahn and J. K. Park, *Lab Chip*, 2011, **11**, 2045–2048.

30 M. A. Hayes, M. M. Petkus, A. A. Garcia, T. Taylor and P. Mahanti, *Analyst*, 2009, **134**, 533–541.

31 Y. Zhang and D. Zhou, *Expert Rev. Mol. Diagn.*, 2012, **12**, 565–571.

32 M. M. Petkus, M. McLauchlin, A. K. Vuppu, L. Rios, A. A. Garcia and M. A. Hayes, *Anal. Chem.*, 2006, **78**, 1405–1411.

33 Y. D. Zhu, J. Peng, L. P. Jiang and J. J. Zhu, *Analyst*, 2014, **139**, 649–655.

34 S. Sakamoto, K. Omagari, Y. Kita, Y. Mochizuki, Y. Maito, S. Kawata, S. Matsuda, O. Itano, H. Jinno, H. Takeuchi, Y. Yamaguchi, Y. Kitagawa and H. Handa, *Clin. Chem.*, 2014, **60**, 610–620.

35 C. F. Woolley and M. A. Hayes, *Bioanalysis*, 2013, **5**, 245–264.

36 Fluorescein-EX Protein Labeling Kit, 2004, http://tools.invitrogen.com/content/sfs/manuals/mp10240.pdf.

37 L. A. Currie, *Anal. Chem.*, 1968, **40**, 586–593.

38 Cardiac Marker ELISA Kits, 2013, http://www.calbiotech.com/products/elisa-kits/human-elisa-kits/cardiac-marker-elisa-kits.

39 Human Heart Fatty Acid Binding Protein ELISA Kit, 2015, http://www.mybiosource.com/prods/ELISA-Kit/Human/Heart-Fatty-Acid-Binding-Protein/H-FABP/datasheet.php?products_id=20502.

40 Plasma Proteome Database, 2014, http://www.plasmaproteomedatabase.org/index.html.

41 P. Mahanti, T. Taylor, M. A. Hayes, D. Cochran and M. M. Petkus, *Analyst*, 2011, **136**, 365–373.

42 E. G. Codding, *Anal. Chem.*, 1979, **51**, 1981–1986.